Journal of Achievements in Materials and Manufacturing Engineering
VOLUME 53
ISSUE 2
August
2012

Thermo-mechanical processing and microstructure evolution of high-manganese austenitic TRIP-type steels

L.A. Dobrzański*, W. Borek, M. Ondrula
Division of Materials Processing Technology, Management and Computer Techniques in Materials Science, Institute of Engineering Materials and Biomaterials, Silesian University of Technology, ul. Konarskiego 18a, 44-100 Gliwice, Poland
* Corresponding e-mail address: leszek.dobrzanski@polsl.pl

Received 12.06.2012; published in revised form 01.08.2012

Materials

ABSTRACT

Purpose: The aim of the paper is to determine the influence of hot-working conditions on microstructure evolution and phase composition of new-developed high-manganese austenitic TRIP-type steels.
Design/methodology/approach: The hot-working behaviour was determined in continuous and multi-stage compression tests performed in a temperature range of 850 to 1100°C by the use of the Gleeble 3800 thermo-mechanical simulator. The processes controlling work hardening and removing it were identified by microstructure evolution observations in different stages of compression with the amount of true strain 4x0.23. Phase composition of steels was confirmed by X-ray diffraction analysis.
Findings: It was found that they have austenite microstructure with numerous annealing twins in the initial state. Continuous compression tests realized in the temperature range from 850 to 1050°C with the strain rate of 0.1, 1 and 10 s^{-1} enabled determination of yield stress values and values of ε_{max} deformations - corresponding to maximum flow stress. The investigated steels are characterized by high values of flow stress from 120 to 380 MPa. Results of the multi-stage compression proved that applying the true strain 4x0.23 gives the possibility to refine the austenite microstructure.
Research limitations/implications: To determine in detail the microstructure evolution during industrial rolling, the hot-working schedule should take into account real number of passes and higher strain rates.
Practical implications: The obtained microstructure - hot-working conditions relationships and stress-strain curves can be useful in determination of power-force parameters of hot-rolling for sheets with fine-grained austenitic structures.
Originality/value: The hot-working behaviour and microstructure evolution in various conditions of plastic deformation for new-developed high-manganese austenitic TRIP-type steels with Nb and Ti microadditions were investigated.
Keywords: High-manganese steel; Hot-working; TRIP-type steels; Dynamic recrystallization; Static recrystallization; Grain refinement

Reference to this paper should be given in the following way:
L.A. Dobrzański, W. Borek, M. Ondrula, Thermo-mechanical processing and microstructure evolution of high-manganese austenitic TRIP-type steels, Journal of Achievements in Materials and Manufacturing Engineering 53/2 (2012) 59-66.

1. Introduction

Today's automotive industry sets very high demands on both production technology and steel used for body of the car, construction elements and other parts of the car. These requirements are the result of continuous improvement of safety standards, which aim to develop a controlled crash area being subject to deformation (damage) according to the scenario, providing maximum absorption of large amounts of impact energy. With proper selection of chemical composition and manufacturing technologies, which guarantee obtaining the structure allowing for connections to provide a favorable strength and plastic properties of steel. In the last three decades have been developed a new group of high-manganese steels with very high strength for use in the automotive industry, which can be divided into TWIP, TRIP and TRIPLEX type steels [1-7].

New-developed steels achieve profitable connection of mechanical properties, i.e. (ultimate tensile strength) UTS~800-1000 MPa, (yield strength) $YS_{0.2}$ = 250-450 MPa, and plastic (uniform elongation) UEl = 35-90%, and moreover, particularly strong formability and strain hardening occurring during forming. The new-developed high-manganese Fe-Mn-(Al, Si) steels provide an extensive potential for automotive industries through exhibiting the twinning induced plasticity (TWIP) and transformation induced plasticity (TRIP) mechanisms. TWIP steels not only show excellent strength, but also have excellent formability due to twinning, thereby leading to excellent combination of strength, ductility, and formability over conventional dual phase steels or transformation induced plasticity TRIP steels. Conditions applied to high-manganese TWIP/TRIP/TRIPLEX steels sheets during deep drawing are different from those applied during tensile testing, the formability cannot be evaluated by mechanical properties obtained from the tensile test. In order to develop automotive steels with excellent properties for CO_2 reduction into the environment and increased efficiency, thus, researches on identifying and understanding these mechanisms are highly required [8-14].

High-manganese TWIP type steel (Twinning Induced Plasticity) is steel, where mechanical twinning is induced by cold plastic deformation. TRIPLEX steels contains 0.7-1.2% C, 18-28% Mn and 8.5 to 12% Al. These steels have a three phase structure consisting of grains of austenite γ-Fe(Mn,Al,C), the dispersion of separating κ-carbide $(Fe,Mn)_3AlC_{1-x}$ and α-Fe ferrite (Mn,Al.). During plastic deformation of the steel in the austenite takes place dislocation slip and mechanical twinning [8]. High manganese TRIP type steels (Transformation Induced Plasticity), contain 0.1 to 0.6% C and 15- 22% Mn, 2-4% Si and 2 to 4% Al. In these steels, TRIP effect is repeated, the transformation of austenite into martensite as a result of cold plastic deformation. TRIP effect consisting in steel hardening in the consequence of $\gamma_{A1} \rightarrow \varepsilon_{A3}$ or $\gamma_{A1} \rightarrow \varepsilon_{A3} \rightarrow \alpha'_{A2}$ martensitic transformation occurring during cold forming. Martensite ε is formed during plastic strain only when stacking fault energy SFE of austenite is lower than 20 mJ/m^2. Addition of aluminium into steel increases SFE and austenite stability which leads to suppressed influence on martensitic transformation. While the addition of silicon decreases SFE and allows occurring of $\gamma \rightarrow \varepsilon$ transformation [1-3, 15-18].

Thermo-plastic treatment applied to form a fine-grained microstructure of austenitic steels used in the automotive industry have to be done in controlled conditions. Using too large deformation, or too long isothermal holding times after the last deformation results in excessive grain refinement of the structure up to about 2 μm, has an impact on increasing strength properties in particular increasing the offset yield point by about 150-200 MPa and tensile strength increase to 1000 MPa [26]. Whereas too large value for the average grain diameter of about 70 μm causes improvement of plastic properties, elongation can achieve even 80-90% at relatively low strength properties. Therefore the main objective of the application of thermo-plastic deformation is the selection of the processing parameters to achieve optimal value for the average grain diameter at which the product of tensile strength and elongation reaches a maximum value. This will allow to increased strain energy per unit volume of structural components of vehicles during traffic collision [19-29].

Application of thermo-mechanical treatment consisting in immediate cooling of products from a finishing temperature of hot-working in controlled conditions should increase mechanical properties [11]. Introduction of Nb and Ti microadditions to one of investigated steel could be the reason for additional strain hardening of high-manganese steels and allows forming a fine-grained microstructure in successive hot-working stages.

2. Materials and experimental procedure

Investigations were carried out on two high-manganese steels X11MnSiAl17-1-3 and X11MnSiAlNbTi18-1-3, containing 17.55-18.25% Mn, 1.17-1.20% Si, 3.29-3.37% Al, and in the case of the second steel - microadditions Nb and Ti. The chemical compositions of steel were shown in Table 1. Steels are characterized by high metallurgical purity, associated with low concentrations of S and P contaminants and gases. Melts were modified with rare earth elements.

Chemical composition of tested steels were chosen in order to obtain the structure of the austenitic matrix. For the investigated melts Nb and Ti microadditions were added in order to refine the structure and achieve precipitation hardening.

Investigated ingots with a mass of 25 kg were performed in a laboratorial vacuum arc furnace of the type VSG-50 from Balzers. Casting of ingots took place in argon atmosphere intended for cast-iron ingot moulds, round with a swage, downwards converging of inner dimensions: bottom - ∅122 mm, top - ∅145 mm, h = 200 mm - without the swage (with the swage – 300 mm). After casting, 60 min were waited, which were required for ingot head to solidify, and subsequently the furnace chamber was opened and further cooling of ingot in the mould took place in the air.

Plastic pre-hot forming of ingots, on a flat bar of 20×220 mm cross-section, was performed by the open die forging method on a high-speed hydraulic press from Kawazoe capable of generating 300 ton pressure. Ingots were heated for forging in a gas forging furnace. The forging temperature ranged between 1200 and 900°C. Subjected to forging were only ingot bodies without ingot heads - cut off at the height to which contraction cavity and ingot feet were reaching - cut off at the height of 3 cm.

Table 1.
Chemical composition of new-developed high-manganese austenitic steels, mass fraction

Steel designation	Chemical composition, mass fraction												
	C	Mn	Si	Al	Nb	Ti	P_{max}	S_{max}	Ce	La	Nd	O	N
X11MnSiAl17-1-3	0.11	17.55	1.17	3.37	-	-	0.002	0.003	0.023	0.007	0.009	0.0003	0.0036
X11MnSiAlNbTi18-1-3	0.11	18.25	1.20	3.29	0.027	0.025	0.002	0.003	0.019	0.005	0.007	0.0004	0.0046

From the pre-forged ingot was prepared test sample. For the purposes of plastometric investigations cylindrical samples Ø10×12 mm were prepared. Continuous compression of samples were made with plastic strain rate equal 0.1, 1 and 10 s^{-1}, in temperature: 1050, 950 and 850°C. In order to simulate thermo-mechanical processing, DSI Gleeble 3800 simulator was used, which allowed for establishing of stress-strain curves of the tested steels and temperature and strain rate influence on processes controlling work hardening of investigated steels.

In the last stage of plastometric examination, a multi-stage compression process was devised for axially symmetric samples, which simulated final roll passes of rolling. The experiment was conducted using also Gleeble 3800 simulator. Reduction ratios, plastic deformation rates and intervals times between successive plastic deformation stages (Fig. 1) were selected taking into account conditions of planned hot rolling of flat bars with initial thickness of 4.5 mm, rolled down to 2 mm thickness samples. Apart from determining force and energy parameters of the hot plastic deformation, the samples were quenched in water, natural cooling in air, and in water after isothermal holding in the temperature of last deformation at 850°C.

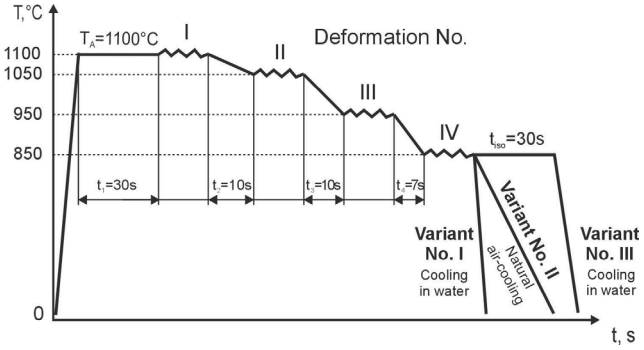

Fig. 1. Schematic and parameters of the multi-stage compression test carried out on Gleeble 3800 thermo-mechanical simulator. T_A - austenitizing temperature, t_{iso} - time of the isothermal holding of specimens at a temperature of last deformation - 850°C

Metallographic examination was carried out on samples in probed steel mounted in thermosetting resins. After the sample was mounted, it was grinded on the STRUERS's grinding machine using abrasive papers of 220-4000 µm/mm^2 grain size. Then the samples were subjected to mechanical polishing using diamond suspension of 6 and 1 µm grain coarseness. In order to reveal grain boundaries in the structure of high-manganese austenitic steels a digestion reagent was used, which was a mixture of nitrous acid, hydrochloric acid and water in 4:4:2 proportions respectively. Also used was a reagent being a mixture of hydrochloric acid, ethyl alcohol and water intended to reveal grain boundaries, as well as deformation bands and ε manganese plates. Digestion time for each sample was ranging between 5-10 s. Structural observations of probed materials were carried out on the LEICA MEF4A light microscope at magnification from 200 to 1000x. X-ray diffraction analysis of specimens in the initial state and after various stages of deformation was carried out using X'Pert PRO diffractometer with the X'Celerator strip detector from Philips, at 0.5° step record and 5 s registration time, using Kα radiation, of λ=1.54056 mm wavelength radiated from copper anode lamp, powered by 40 kV voltage at 30 mA filament current. Measurements were taken within the radial range from 20 to 140°. Identification of phases was completed based on data available in the database of Centre for Diffraction Data (ICDD).

3. Results and discussion

Starting points for microstructure analysis of specimens that were plastically hot-deformed in variable conditions are microstructures in the initial state of the investigated steels X11MnSiAl17-1-3 and X11MnSiAlNbTi18-1-3 (Figs. 2, 4). Minor differences between chemical composition of elaborated steels result in meaningful difference of a grain size in the initial state. Steel X11MnSiAl17-1-3 is characterized by homogeneous microstructure of austenite with a grain size in range from 150 to 200 µm (Fig. 2). In steel X11MnSiAlNbTi18-1-3 Nb and Ti microadditions has an impact on reducing the mean grain size up to about 50-60 µm (Fig. 4). Application of Nb and Ti microadditions has influence on significant structure refinement and hampering influence of growth of grains size of austenite. In both investigated steels numerous annealing twins can be observed (Figs. 2, 4). Single-phase microstructure of both investigated steels was confirmed by X-ray diffraction pattern (Figs. 3, 5).

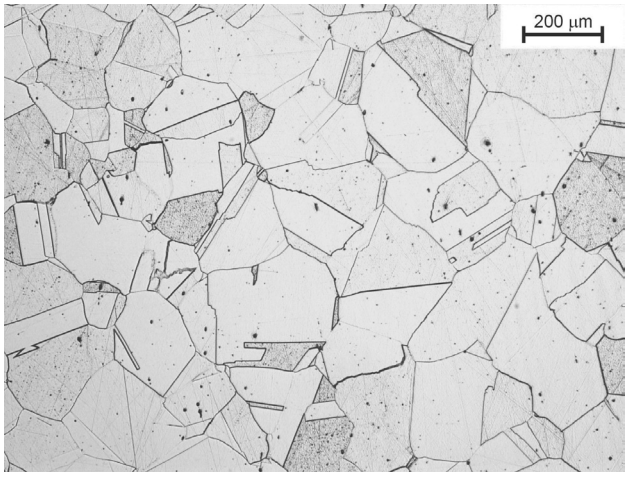

Fig. 2. Austenitic structure of the X11MnSiAl17-1-3 steel containing annealing twins and some non-metallic inclusions

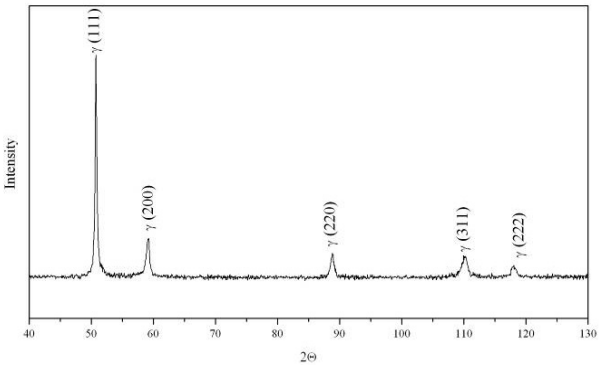

Fig 3. X-ray diffraction pattern of the investigated steel X11MnSiAl17-1-3 in the initial state

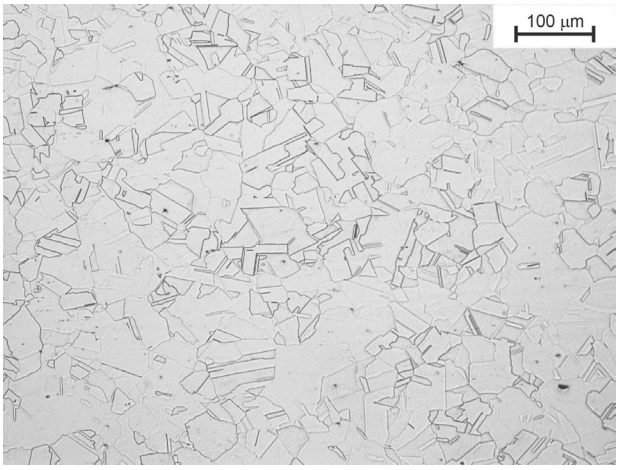

Fig. 4. Austenitic structure of the X11MnSiAlNbTi18-1-3 steel containing annealing twins and some non-metallic inclusions

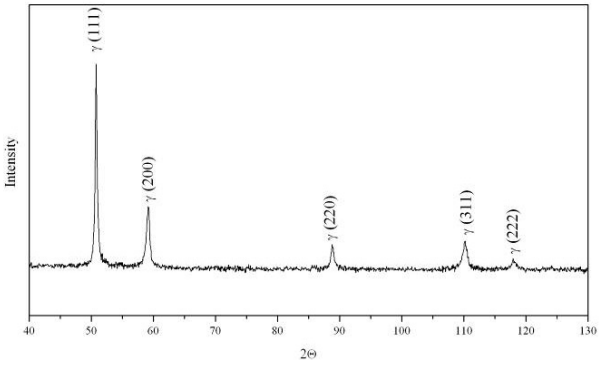

Fig 5. X-ray diffraction pattern of the investigated steel X11MnSiAlNbTi18-1-3 in the initial state

The stress-strain curves of the X11MnSiAl17-1-3 and X11MnSiAlNbTi18-1-3 steels determined in continuous hot-compression test in various conditions of temperature and strain rate are shown respectively in Figs. 6 and 7 indicate, that strain rate has an essential influence on value of flow stress. Steel X11MnSiAl17-1-3 is characterized by values of flow stress equal from 120 to 360 MPa and for steel X11MnSiAlNbTi18-1-3 values of flow stress are equal from 130 to 380 MPa for applied deformation conditions. Increasing temperature of deformation or decreasing strain rate cause decreasing relatively high values of flow stress. Along with strain temperature decreasing, the value of ε_{max} - corresponding to the maximum value of yield stress - is translating to a range of higher deformations. For steel X11MnSiAl17-1-3 the values of ε_{max} for samples deformed at rate of 0.1 s^{-1} at the temperature 1050°C is equal about 0.35 and increase up to 0.59 with decreasing the temperature to 850°C and increasing strain rate up to 10 s^{-1}. Whereas for steel X11MnSiAlNbTi18-1-3 with Nb and Ti micro-additions value of ε_{max} for applied deformation conditions increases from 0.2 to 0.52. It creates convenient conditions for using dynamic recrystallization for refinement of microstructure of investigated steels.

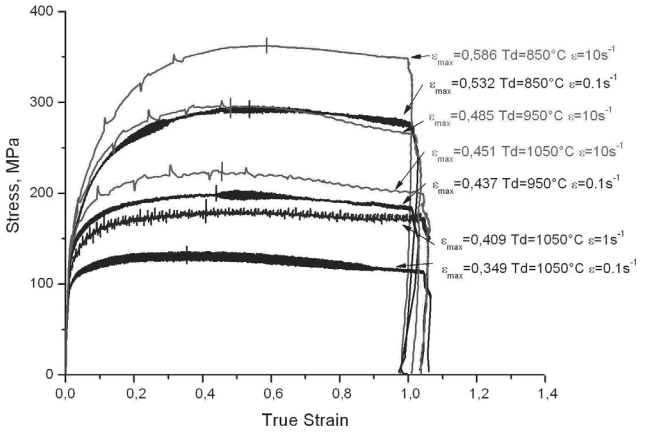

Fig. 6. Stress-strain curves of the X11MnSiAl17-1-3 steel obtained for different strain rate: 0.1, 1, 10 s^{-1}, and in a temperature: 850, 950 and 1050°C

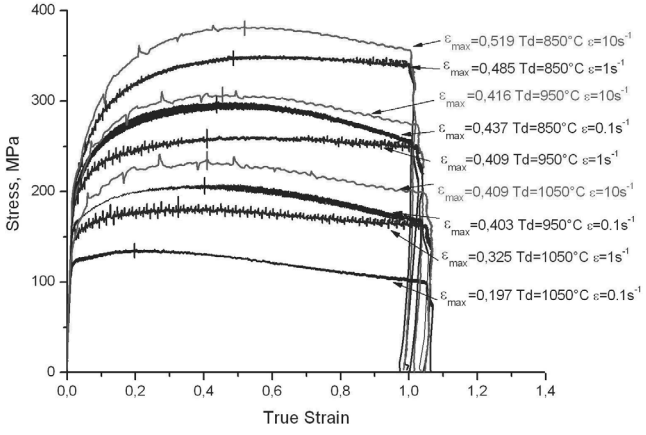

Fig. 7. Stress-strain curves of the X11MnSiAlNbTi18-1-3 steel obtained for different strain rate: 0.1, 1, 10 s^{-1}, and in a temperature: 850, 950 and 1050°C

The fraction of the recrystallized phase in intervals between successive passes for steel X11MnSiAlNbTi18-1-3 can be

evaluated from Fig. 8, showing results of softening kinetics of austenite in intervals between first and second stage of plastic deformations. Progress of recrystallization as a function of time for the specimens compressed at the temperature 900°C with strain rate equal $10s^{-1}$ indicate that time necessary to form 50% fraction of recrystallized austenite is equal approximately 8 s. Time needed to reach total recrystallization for steel X11MnSiAlNbTi18-1-3 compressed at the temperature 900°C with strain rate equal 10 s^{-1} is approximately 300-400 s.

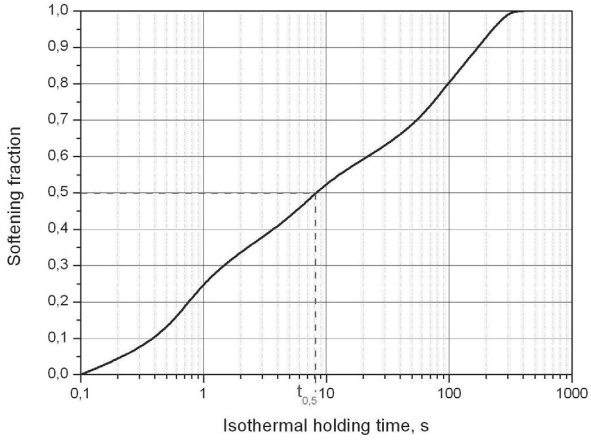

Fig. 8. Progress of recrystallization of the X11MnSiAlNbTi18-1-3 steel isothermally held after plastic deformation compressed at the temperature 900°C with strain rate equal 10 s^{-1}

Stress-strain curves of steels plastically deformed according to the parameters shown in Fig. 1 are presented in Fig. 9. Multi-stage work-hardening curves of two new-developed high-manganese TRIP steels (Fig. 9) can be useful to estimate force-energetic parameters of industrial hot rolling. Application of true strain equal 0.23 during four-stage compression creates possibility of the course of dynamic recrystallization, which is indicated by peaks that can be distinguished on σ-ε curves, especially for deformations realized at temperature of 1100, 1050 and 950°C. The values of flow stress in the range of strain temperature from 1100 to 1050°C (Fig. 9) are comparable with values obtained in continuous compression test with the strain rate 10 s^{-1} (Figs. 6, 7). Significant decrease of flow stress by about 40-50 MPa is noted for the third step of deformation realized at the temperature of 950°C. In the final deformation at the temperature 850°C values of flow stress are equal approximately 320 MPa which is about 40 and 50 MPa lower than the values obtained for the continuous compression tests at the temperature of 850°C with the strain rate $10s^{-1}$ respectively for investigated steels X11MnSiAl17-1-3 and X11MnSiAlNbTi18-1-3. It's a result of partial removal of strain hardening through metadynamic recrystallization that occurs during the intervals between second, third and fourth deformation. Additionally, cyclic deformations as well as the course of partial recrystallization result in much faster achievement of maximum on σ-ε curve for the fourth deformation when comparing to σ-ε curve of continuous compression at the temperature of 850°C.

Some of the typical optical micrographs of high-manganese austenitic X11MnSiAl17-1-3 and X11MnSiAlNbTi18-1-3 steels after hot working in the thermo-mechanical simulator Gleeble 3800 are shown respectively in Figs. 10 and 11. Solution heat treatment of X11MnSiAl17-1-3 steel in water directly after last deformation causes significant refinement of structure in consequences of dynamic recrystallization especially during first and second stage of deformations. After last deformation of the specimen at a temperature of 850°C and subsequent cooling in water, the steel is characterised by uniform, austenite microstructure with a mean grain size of about 20-25 μm (Fig. 10a). The initiation of metadynamic and static recrystallization after the last deformation and subsequent air-cooling leads to obtain mean grain size of about 20 μm (Fig. 10b). Isothermal holding of the steel X11MnSiAl17-1-3 after the last deformation at 850°C for 30 s leads to growth of new grains as a result of metadynamic recrystallization and the initiation of static recrystallization (Fig. 10c). Mean austenite grain size after this variant of thermo-mechanical treatment is about 10-12 μm. Application of different variants of thermo-mechanical treatment has no influence on stability of austenite. Confirmation of that fact is the X-ray diffraction patterns shown in Fig. 12 for X11MnSiAl17-1-3 steel which presents the comparison of diffraction after different stages of thermo-mechanical treatment. Is connected with significant structure refinement and hampering influence of grain boundaries of austenite.

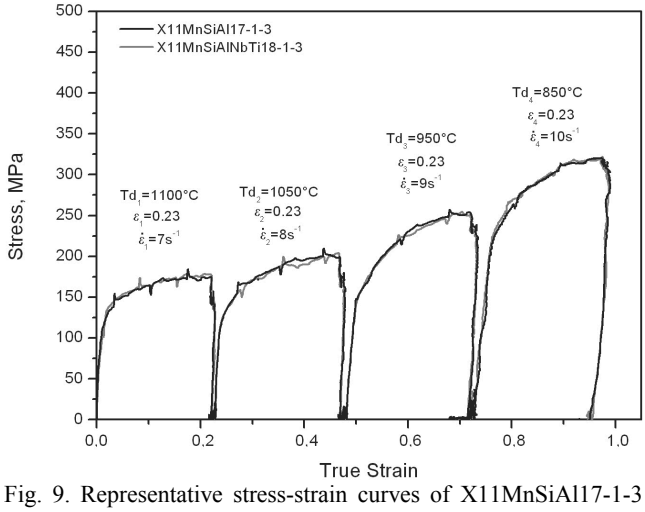

Fig. 9. Representative stress-strain curves of X11MnSiAl17-1-3 and X11MnSiAlNbTi18-1-3 steels after multi-stage compression axially symmetrical specimens deformed in a temperature range from 1050 to 850°C according to the scheme shown in Fig. 1

Structures of X11MnSiAlNbTi18-1-3 steel after thermo-mechanical treatment are presented in Fig. 11. After final deformation at temperature 850°C and subsequent cooling in water, steel characterise uniform structure with grains size about 25 to 30 μm (Fig. 11a). Air-cooling after last deformation no cause significant changes in microstructure (Fig. 11b). Appling isothermal holding of specimens at 850°C for 30 s leads to obtain mean grain size of about 8-12 μm (Fig. 11c) as a result of metadynamic and static recrystallization. Investigated X11MnSiAlNbTi18-1-3 steel keeps stable austenite microstructure independently from conditions of hot-plastic deformation, what was confirmed by X-ray diffraction pattern shown in Fig. 13.

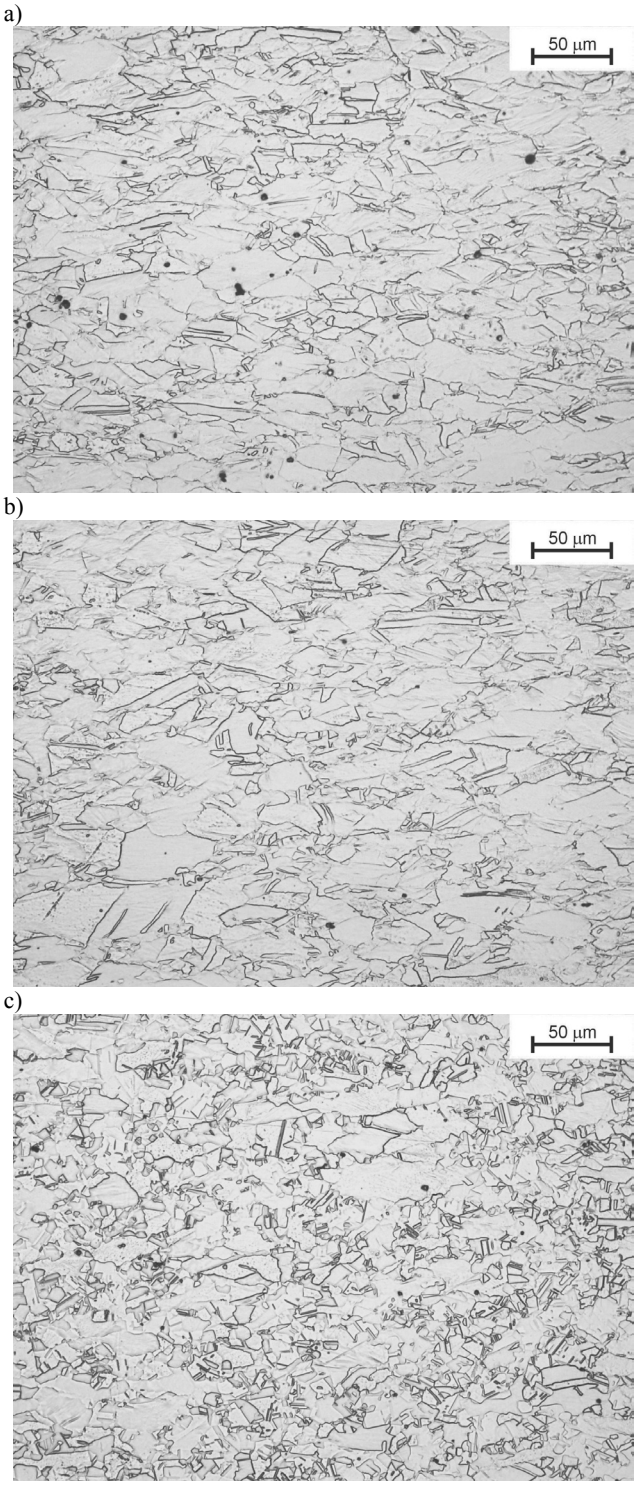

Fig. 10. Microstructures of high-manganese austenitic X11MnSiAl17-1-3 steel after thermo-mechanical processing according to schedule shown in Fig. 1, and cooling from temperature of last deformation at 850°C b) in water, c) air-cooling, d) in water after isothermal holding 30 s at 850°C

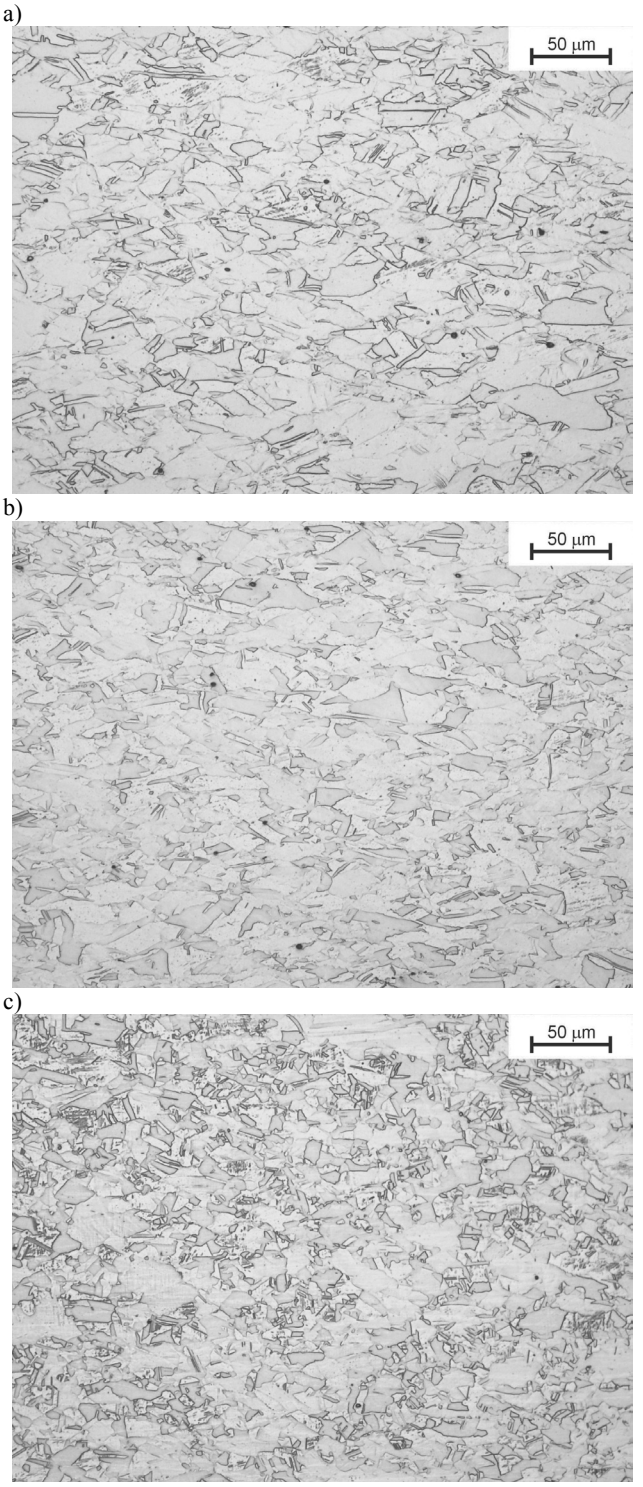

Fig. 11. Microstructures of high-manganese austenitic X11MnSiAlNbTi18-1-3 steel after thermo-mechanical processing according to schedule shown in Fig. 1, and cooling from temperature of last deformation at 850°C b) in water, c) air-cooling, d) in water after isothermal holding 30 s at 850°C

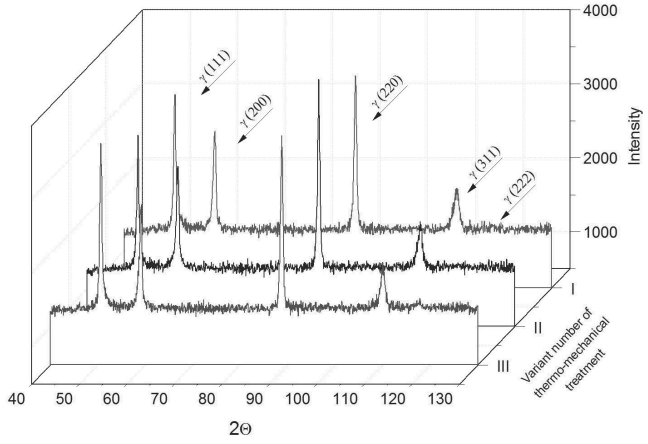

Fig. 12. X-ray diffraction patterns for X11MnSiAl17-1-3 steel after various variants of the thermo-mechanical treatment according to the scheme shown in Fig. 1

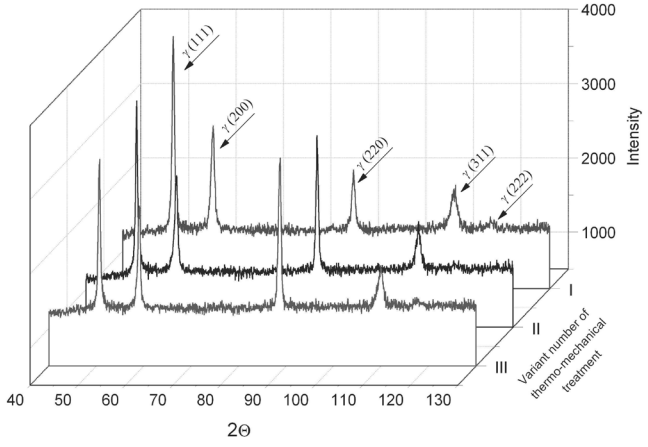

Fig. 13. X-ray diffraction patterns for X11MnSiAlNbTi18-1-3 steel after various variants of the thermo-mechanical treatment according to the scheme shown in Fig. 1

4. Conclusions

The differences in chemical composition don't have meaningful influence on behaviour of these steels in conditions of hot-working. Steel X11MnSiAl17-1-3 is characterized by homogeneous microstructure of austenite with a grain size in range from 150 to 200 μm. Application of Nb and Ti microadditions in second steel has an impact on reducing the mean grain size up to about 50-60 μm. Nb and Ti microadditions has influence on significant structure refinement and hampering influence of growth of grains size of austenite in the initial state. Elaborated steels are characterized by relatively high values of flow stress, equal from 120 to 380 MPa, and values of ε_{max} deformation come from a range from 0.20 to 0.57, corresponding to maximum value of yield stress. Small values of ε_{max} allow to obtain a fine-grained microstructure due to the dynamic recrystallization. The refinement of the austenite microstructure during intervals between successive stages of deformation is caused by metadynamic recrystallization, whereas the fine-grained microstructure of the steel after the last deformation at a temperature of 850°C is a result of dynamic recrystallization. Further refinement of the microstructure can be obtained by isothermal holding of the specimens in a finishing hot-working temperature for 30 s. Applied thermo-mechanical treatment allowed to obtain refinement of steel structure with a grains size up to about 8-10 μm. Repeated recrystallization and corresponding grain refinement causes that the thermo-mechanically processed steel is characterized by uniform structure. The fine-grained structure has influence on a phase composition of steel and should increase mechanical properties during subsequent cold plastic deformations.

Acknowledgements

Scientific work was partially financed from the science funds in a period of 2009-2011 in the framework of project No. N N507 287936 headed by Prof. L.A. Dobrzański.

The authors would like to express their gratitude to Prof. R. Kuziak of Institute for Ferrous Metallurgy in Gliwice for carrying out the experiments using the Gleeble 3800 simulator.

References

[1] G. Frommeyer, U. Brüx, K. Brokmeier, R. Rablbauer, Development, microstructure and properties of advanced high-strength and supraductile light-weight steels based on Fe-Mn-Al-Si-(C), Proceedings of the 6th International Conference "Processing and Manufacturing of Advanced Materials" Thermec'2009, Berlin, 2009, 162.

[2] G. Frommeyer, U. Brüx, P. Neumann, Supra-ductile and high-strength manganese-TRIP/TWIP steels for high energy absorption purposes, Iron and Steel Institute of Japan International 43 (2003) 438-446.

[3] O. Grässel, L. Krüger, G. Frommeyer, L.W. Meyer, High strength Fe-Mn-(Al, Si) TRIP/TWIP steels development - properties - application, International Journal of Plasticity 16 (2000) 1391-1409.

[4] J.A. Jiménez, G. Frommeyer, Analysis of the microstructure evolution during tensile testing at room temperature of high-manganese austenitic steel, Materials Characterization 6 (2010) 221-226.

[5] R. Kuziak, R. Kawalla, S. Waengler, Advanced high strength steels for automotive industry, Archives of Civil and Mechanical Engineering 8/2 (2008) 103-117.

[6] O. Bouaziz, S. Allain, C.P. Scott, P. Cugy, D. Barbier, High manganese austenitic twinning induced plasticity steels: A review of the microstructure properties relationships, Current Opinion in Solid State and Materials Science 15 (2011) 141-168.

[7] Z. Gronostajski, A. Niechajowicz, S. Polak, Prospects for the use of new-generation steels of the ahss type for collision energy absorbing components, Current Opinion in Solid State and Materials Science 15 (2011) 141-168.

[8] S. Vercammen, B. Blanpain, B.C. De Cooman, P. Wollants, Mechanical behaviour of an austenitic Fe-30Mn-3Al-3Si and the importance of deformation twinning, Acta Materialia 52 (2004) 2005-2012.
[9] A. Grajcar, W. Borek, The thermo-mechanical processing of high-manganese austenitic TWIP-type steels, Archives of Civil and Mechanical Engineering 8/4 (2008) 29-38.
[10] L.A. Dobrzański, A. Grajcar, W. Borek, Microstructure evolution and phase composition of high-manganese austenitic steels, Journal of Achievements in Materials and Manufacturing Engineering 31/2 (2008) 218-225.
[11] L.A. Dobrzański, W. Borek, Hot-working of advanced high-manganese austenitic steels, Journal of Achievements in Materials and Manufacturing Engineering 43/2 (2010) 507-526.
[12] L.A. Dobrzański, W. Borek, Hot-Working Behaviour of Advanced High-Manganese C-Mn-Si-Al Steels, Materials Science Forum 654-656 (2010) 266-269.
[13] L.A. Dobrzański, W. Borek, Microstructure forming processes of the 26Mn-3Si-3Al-Nb-Ti steel during hot-working conditions, Journal of Achievements in Materials and Manufacturing Engineering 40/1 (2010) 25-32.
[14] L.A. Dobrzański, W. Borek, Hot-working of advanced high-manganese austenitic steel, Journal of Achievements in Materials and Manufacturing Engineering 43/2 (2010) 507-526.
[15] L.A. Dobrzański, W. Borek, Hot deformation and recrystallization of advanced high-manganese austenitic TWIP steels, Journal of Achievements in Materials and Manufacturing Engineering 46/1 (2011) 71-78.
[16] L.A. Dobrzański, W. Borek, Hot-rolling of high-manganese Fe - Mn - (Al, Si) TWIP steels, Proceedings of 8th International Conference "Industrial Tools and Material Processing Technologies" ICIT&MPT'2011, Slovenia, 2011, 117-120.
[17] L.A. Dobrzański, W. Borek, Hot-rolling of advanced high-manganese C-Mn-Si-Al steels, Materials Science Forum 706-709 (2012) 2053-2058.
[18] N. Cabanas, N. Akdut, J. Penning, B.C. De Cooman, High-temperature deformation properties of austenitic Fe-Mn alloys, Metallurgical and Materials Transactions A 37 (2006) 3305-3315.
[19] A. Grajcar, M. Opiela, G. Fojt-Dymara, The influence of hot-working conditions on a structure of high-manganese steel, Archives of Civil and Mechanical Engineering 9/3 (2009) 49-58.
[20] A. Grajcar, Hot-working in the γ+α region of TRIP-aided microalloyed steel, Archives of Materials Science and Engineering 28/12 (2007) 743-750.
[21] J. Adamczyk, A. Grajcar, Heat treatment and mechanical properties of low-carbon steel with dual-phase micro-structure, Journal of Achievements in Materials and Manufacturing Engineering 22/1 (2007) 13-20.
[22] J. Adamczyk, A. Grajcar, Structure and mechanical properties of DP-type and TRIP-type sheets, Journal of Materials Processing Technology 162-163 (2005) 267-274.
[23] A. Grajcar, Effect of hot-working in the γ+α range on a retained austenite fraction in TRIP-aided steel, Journal of Achievements in Materials and Manufacturing Engineering 22/2 (2007) 79-82.
[24] K.T. Park, K.G. Jin, S.Ho Han, S. Woo Hwang, K. Choi, C. Soo Lee, Stacking fault energy and plastic deformation of fully austenitic high manganese steels: Effect of Al addition, Materials Science and Engineering A 527 (2010) 3651-3661.
[25] A. Grajcar, Selection of the hot-working conditions for TRIP-type microalloyed steel, Archives of Materials Science and Engineering 31/2 (2008) 75-78.
[26] G. Dini, A. Najafizadeh, R. Ueji, S.M. Monir-Vaghefi, Tensile deformation behavior of high manganese austenitic steel: The role of grain size, Materials and Design 31 (2010) 3395-3402.
[27] R.F. Kuble, M. Berveiller, P. Buessler, Semi phenomenological modelling of the behavior of TRIP steels, International Journal of Plasticity 27 (2011) 299-327.
[28] A. Weidner, S. Martin, V. Klemm, U. Martin, H. Biermann, Stacking faults in high-alloyed metastable austenitic cast steel observed by electron channelling contrast imaging, Scripta Materialia 64 (2011) 513-516.
[29] F. Lu, P.Yang, L. Meng, F. Cui, H. Ding, Influences of Thermal Martensites and Grain Orientations on Strain-induced Martensites in High Manganese TRIP/TWIP Steels, Journal of Materials Science and Technology 27/3 (2011) 257-265.